Pergamon

Int. J. Heat Mass Transfer. Vol. 39, No. 14, pp. 2907–2913, 1996

0017-9310/96 $15.00 + 0.00

0017-9310(95)00383-5

Flow and heat transfer measurements of a wall attaching offset jet

DAE SEONG KIM and SOON HYUN YOON
Department of Mechanical Design Engineering, Research Institute of Mechanical Technology, Pusan National University, Pusan, 609-735, Korea

DAE HEE LEE†
Department of Mechanical Engineering, Inje University, Obang-Dong, Kimhae, 621-749, Korea

and

KYUNG CHUN KIM
Department of Mechanical and Production Engineering, Research Institute of Mechanical Technology, Pusan National University, Pusan, 609-735, Korea

(*Received* 27 *July* 1995 *and in final form* 24 *October* 1995)

Abstract—An experimental study on the fluid flow and heat transfer characteristics was performed for a two-dimensional jet issuing parallel to a flat plate. A split film probe and thermochromic liquid crystal are used to measure the mean velocity and turbulent intensity, and plate wall temperature, respectively. The offset ratio ranges from 0 to 20, the Reynolds number from 6500 to 39 000 and the nozzle width is 20 mm. It is observed that a dividing streamline of the jet unstably reattaches in the impingement region. However, the time-averaged reattachment points are found to coincide with the maximum Nusselt number locations. The correlations between the local Nusselt number distributions and Reynolds number Re, offset ratio H/D, and streamwise length X/D are presented. Copyright © 1996 Elsevier Science Ltd.

INTRODUCTION

When a plane jet is issued into quiescent surroundings above a plate parallel to the axis of the jet discharge, the so-called "coanda effect" forces the jet to deflect towards the wall boundary and attach to the plate wall. After the jet impinges on the wall, the flow redevelops in the wall jet region. The general flow field in the Wall Attaching Offset Jet (WAOJ) is schematically depicted in Fig. 1.

WAOJ is frequently found in many engineering devices such as the cooling of a combustion chamber wall in a gas turbine, the use of an air deflector as a circulation controller, and an automobile demister. Early works by Borque and Newmann [1] and Sawyer [2] have been concerned mostly with the mean flow characteristics. Hoch and Jiji [3] presented an integral analysis on the basis of an entrainment model which predicts the jet trajectory, the reattachment length, the wall pressure distribution, and the maximum axial velocity decay. Pelfray and Liburdy [4] provided the detailed experimental data for the mean and turbulent velocity fields in the recirculation and impingement regions. Recently, Yoon *et al.* [5] presented the turbulent data in the entire region of WAOJ ranging from the recirculation region to the wall jet region.

Although many investigations on WAOJ have been presented, the studies on both the flow and heat transfer characteristics of the WAOJ are scarce. A few researchers have investigated the heat or mass transfer characteristics of the WAOJ. Kumuda *et al.* [6] measured the mass transfer coefficients in the WAOJ using the naphthalene sublimation technique. They reported that a change of the recirculation bubble shape occurred when the offset ratio, H/D, becomes greater than 6.5. Hoch and Jiji [7] studied the thermal characteristics and heat decay phenomena of the heated WAOJ and concluded that the temperature distributions in the recirculation bubble are uniform. Holland and Luburdy [8] investigated the temperature and energy distributions of the heated WAOJ under the adiabatic wall condition and presented that the buoyant effects on the WAOJ are negligible. They also compared their thermal data with the flow field structure provided by Pelfray and Liburdy [4].

The present study is aimed at investigating the fluid flow and heat transfer characteristics of the WAOJ. The mean velocities, turbulent intensities, and local convective heat transfer coefficients in the entire region of the WAOJ are measured by employing a split film probe and thermochromic liquid crystal.

† Author to whom correspondence should be addressed.

NOMENCLATURE

D	nozzle width
H	distance from the wall to the lower nozzle edge
h	local convection heat transfer coefficient
k	thermal conductivity
Nu	local Nusselt number, hD/k
Nu_{max}	maximum Nusselt number
Nu_{stag}	stagnation point Nusselt number
q	heat flux
Re	Reynolds number (based on the nozzle width, D)
T	temperature
U_J	jet velocity at the nozzle exit
u', v', w'	velocity fluctuation components
X_{max}	maximum Nusselt number position
X_{min}	minimum Nusselt number position
X_R	reattachment distance
X^+	dimensionless axial coordinate $=(X-X_{max})/X_{max}$
X, Y	horizontal and vertical coordinate
$Y_{1/2m}$	upper jet spread.

Greek symbols

ε	emissivity
γ	forward flow fraction
ν	kinematic viscosity
σ	Stefan–Boltzmann constant.

Subscripts

a	ambient
c	conduction
J	jet
v	convection
w	offset wall.

EXPERIMENTAL APPARATUS

Measurements are made in a low speed blow-down wind tunnel. Air is moved by 5HP centrifugal fan and the fan speed is controlled by an inverter. The wind tunnel consists of a diffuser, plenum chamber and a contraction nozzle. It has a contraction ratio of 25 and a size of the exit nozzle is 800 mm × 20 mm, resulting in an aspect ratio of 40. The jet velocity, U_J, is measured with a pitot tube and electronic micro manometer to an accuracy of $\pm 2\%$. The initial turbulent intensities at the nozzle exit are $u'/U_J = 0.1\%$, $v'/U_J = 0.2\%$ and $w'/U_J = 0.15\%$, respectively.

The test plate on which the discharged jet attaches is made of a 800 mm high, 2 m long and 10 mm thick Plexiglas. The test plate is installed such that it is parallel to the jet streamwise axis and vertical to the plate which is flush with the end of nozzle.

In order to minimize the conduction heat loss, a gypsum plate is placed above the Plexiglas plate. To the surface of the gypsum plate is glued a sheet of gold film Intrex (a very thin gold-coated polyester substrate

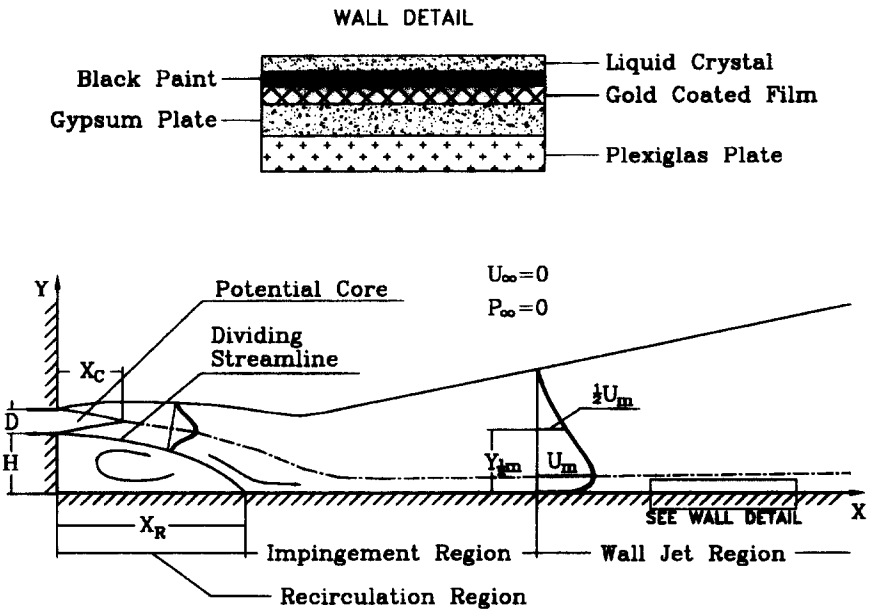

Fig. 1. Schematic diagram of the wall attaching offset jet flow experiment.

sheet). Copper foil strip "electrodes" are then attached to either end of the surface of the Intrex and silver-loaded paint is applied to establish a good electrical contact between the copper electrodes and the Intrex surface. By passing a d.c. current through the Intrex, an essentially uniform wall heat flux boundary condition is created. The copper electrodes are then connected to two digital multimeters with a precision of three significant figures to measure the voltage drop across and current input to the Intrex.

An air brush connected to an air compressor was used to apply first black backing paint and then the liquid crystal on the Intrex surface. The liquid crystal used in this experiment is "R35C1W" micro-encapsulated thermochromic liquid crystal.

In order to minimize the conduction and radiation heat losses, care was taken; the backside of the Intrex was well insulated with the gypsum plate and a fiber optic cold light source was used to illuminate the liquid crystal surface. Since the actual color image is affected by factors such as the angle and distance of the light illuminating the liquid crystal covered surface, and aging effects, a careful color calibration was carried out. In order to accurately determine the spatial location of the particular color and to minimize a visual bias, a true color image processing system was used.

All of the flow measurements were made for a Reynolds number of $Re = 39\,000$ and an offset ratio of $H/D = 5.0$ except for forward flow fractions. Heat transfer measurements were made over a range of Reynolds numbers from 6500 to 39 000, and the offset ratios ranging from 0.5 to 15.

DATA REDUCTION

Details of the flow and heat transfer measurement technique used in this study are described by Yoon [9] and Lee *et al.* [10], respectively. And the hue-temperature correlation used for the liquid crystal calibration is presented by Kim [11].

For the accurate measurement of the complex flow field in the WAOJ, a split film probe (TSI-1288) which is an end-flow-type, 0.15 mm diameter and 2 mm long, was used. This probe was calibrated at the exit of the round jet issuing from the nozzle of TSI-1125 calibrator. In the present study, the modified Stock's calibration scheme proposed by Ra *et al.* [12] was modified to improve the pitch angle response for the flow velocity variation. The uncertainty estimates by the Kline and McKlintock's [13] method show that the uncertainty in the mean velocity at the maximum pitch angle of above $\pm 70°$ is less than 5%.

A location of the reattachment point was estimated by a forward flow fraction, γ_w, which is defined as a fraction of time duration during which the flow is directed towards downstream. The streamwise and crosswise turbulent velocity components in the WAOJ were measured using two constant temperature anemometers (TSI, IFA100). The anemometer output signals were low pass filtered at 5 kHz through two TSI-1057 signal conditioners, then digitized by a universal waveform analyzer (Data Precision, D6000) which has a 14 bit A/D converter with a sampling frequency of 10 kHz.

A calibrated 0.025 cm diameter chromel–alumel thermocouple measured the jet exit temperature to an accuracy of $\pm 0.1°C$. By electrically heating a very thin gold-coating on the Intrex, an essentially uniform wall heat flux condition is established. The heat flux can be adjusted by changing the current through the Intrex, which changes the surface temperature. Under the constant heat flux condition, an isotherm on the Intrex surface corresponds to a contour of a constant heat transfer coefficient. As the heat flux changes, the position of the color isotherm is also moved. The local heat transfer coefficient at the position of the particular color being observed is calculated from

$$h = \frac{q_v}{(T_w - T_j)} \tag{1}$$

where T_w is the wall temperature determined by liquid crystal, T_j is the jet temperature, q_v is the net heat flux which is obtained by subtracting the heat losses from the total heat flux through the Intrex, i.e.

$$q_v = \frac{fIV}{A} - \varepsilon\sigma(T_w^4 - T_a^4) - q_c. \tag{2}$$

The ratio of the local electrical heating to the average heating, f is a measure of the uniformity of the gold coating. Baughn *et al.* [14] found the uniformity to be as high as 98% when the test section of Intrex is small and selected from the middle of a roll where the gold-coating is most uniform. It has been the case for the present experiment. Therefore, we assume $f = 1$ for the heat flux calculation, but f is maintained in equation (2) because it contributes to the overall uncertainty (see Table 1). The variables I, V, A, ε, σ, T_a and q_c are the current across the Intrex, voltage across the Intrex, surface area of the Intrex, emissivity of liquid crystal on the surface of the plate, Stefan–Boltzmann constant, ambient temperature and the conduction loss, respectively. The uncertainty estimates using the method suggested by Kline and McKlintock [13] show that the Nusselt number un-

Table 1. Nusselt number uncertainty analysis

x^i	Unit	Value	δx_i	$\frac{\delta x_i}{Nu}\frac{\partial Nu}{\partial x_i} \times 100\,(\%)$
f		1.0	0.02	1.97
A	[m^2]	0.0025	4.975×10^{-5}	1.90
T_w	[°C]	35.6	0.22	1.56
V	[V]	11.291	0.125	1.06
I	[A]	0.45	5.0×10^{-3}	1.06
T_a	[°C]	21.2	0.14	0.93
D	[m]	0.02	5.0×10^{-5}	0.23
ε		0.9	0.05	0.21

Total Nu uncertainty: $\frac{\delta Nu}{Nu} = 3.59\%$.

certainty for $H/D = 5$ and $X/D = 12$ at $Re = 39\,000$ is 3.59%. The uncertainty in the gold coating uniformity factor is the largest contribution to the uncertainty. Another source of the large uncertainty is the measurement of the Intrex area.

RESULTS AND DISCUSSION

Flow characteristics

Figure 2 shows variations of the downstream distance from the jet exit to the reattachment, X_R, with the offset ratio, H/D, for $Re = 39\,000$. A majority of previous investigators have used the reattachment point as an important parameter to better understand the flow characteristics of the WAOJ. However, the WAOJ flow reattachment is a very unsteady process and flow visualization experiments using tufts reveal that the reattachment region is rather wide. In spite of the unsteadiness of the reattachment distance, it can be estimated from Fig. 2. The point where the mean skin friction coefficient vanishes (i.e. the γ_w value becomes 0.5) is considered as the time-averaged reattachment point of the unsteady reattaching flow as suggested by Yoon *et al.* [5]. It is shown that the reattachment length increases with an increasing offset ratio. It is also shown that the reattachment distances for the present experiment are slightly larger than those of Borque and Newmann [1] and Sawyer [2]. But a linear dependence of the reattachment distance on the offset ratio is consistent with that of the dimensional analysis of Borque and Newmann [1]. The wall reattaching region normalized by the reattachment distance is plotted against the offset ratio in Fig. 3. The graph shows a slight asymmetry about the time-averaged reattachment point (i.e. $\gamma_w = 0.5$). This asymmetry may be due to a developing nature of the issuing jet from the nozzle. It appears that the minimum reattachment region occurs in the vicinity of $H/D = 7$, which agrees with the result by Kumada *et al.* [6]. Kumada *et al.* [6] have suggested that variations of flow and mass transfer characteristics occur around $H/D = 6.5$.

The mean velocity vector profiles in the initial flow development region of the WAOJ for $H/D = 5.0$ are shown in Fig. 4. From this figure, the recirculation region is readily observed with the cortex center located at $X/D \approx 7$. The existence of a secondary vortex flow is in evidence in the corner at which the offset plate and the back wall intersect. The primary jet flow appears to gradually curve through the first one third of the recirculating region and turns sharply downward as the jet impinges on the plate. This trend has also been observed in the backward facing step flows, but the streamline started to curve after one half of the recirculation bubble. In the present experiment, the maximum reverse flow velocity was about 27% of the jet exit velocity.

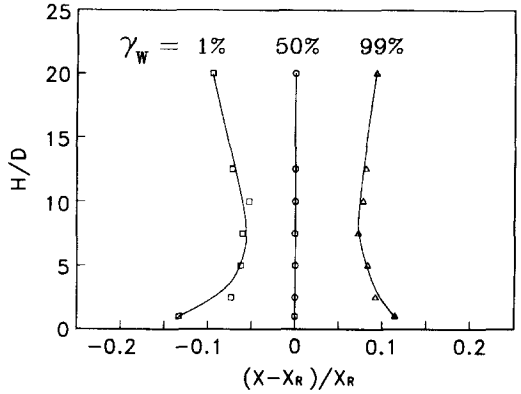

Fig. 3. Variations of the reattachment region with offset ratio for $Re = 39\,000$.

To investigate similarities in the flow characteristics between the WAOJ and the plane wall jet (PWJ) in the far downstream region, the mean velocity profiles for both cases are plotted against the vertical distance in Fig. 5. According to Rajaratnam and Subramanya [15] who performed the plane turbulent attached wall jet experiments, the mean velocity profiles in the wall jet region become similar for $X \geqslant 20D$. A similar behavior is also observed in the WAOJ experiments for $X > 20D$ in Fig. 5.

Variations of the turbulent intensity profiles, u'/U_j and v'/U_j, are shown in Fig. 6. Due to a violent mixing

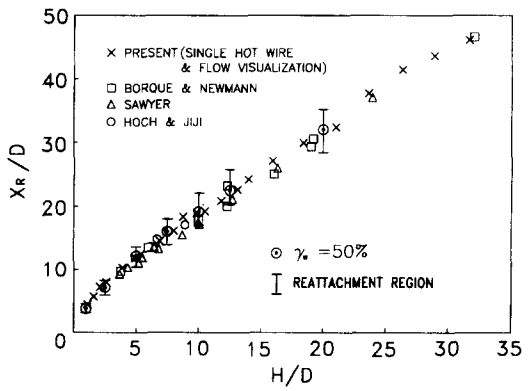

Fig. 2. Variations of the reattachment length with offset ratio for $Re = 39\,000$.

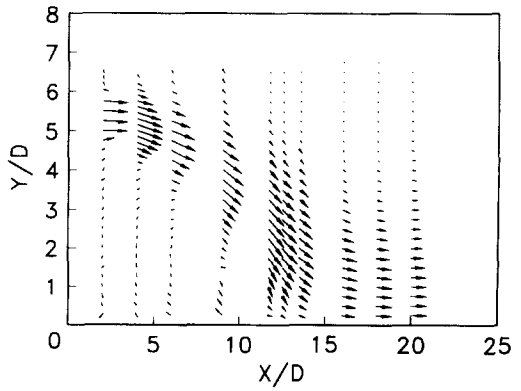

Fig. 4. Mean velocity vector profiles in the WAOJ for $H/D = 5.0$ and $Re = 39\,000$.

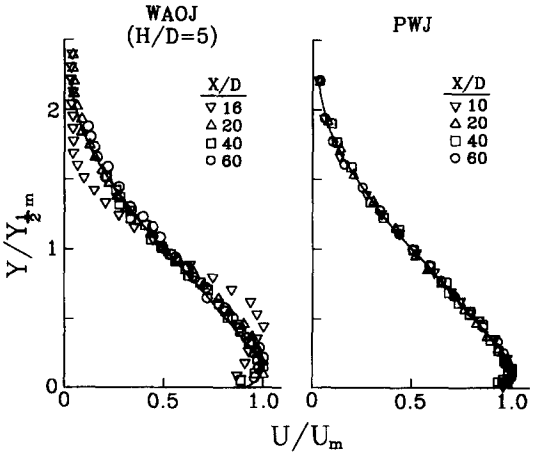

Fig. 5. Mean velocity profiles in the WAOJ and the PWJ for $Re = 39\,000$.

process of the discharged jet with surroundings, both components have a sharp peak on each side at $X/D \approx 1$. Such peaks persist until $X/D \approx 20$ and disappear in the wall jet region. Due to a suction pressure in the recirculation region, the upper profiles skew toward the bottom plate. It is worth noting that values of v'/U_J are higher in the lower region than in the upper region of the jet. This is attributed to a direct production mechanism of the vertical turbulent component by the curvature field in the recirculation region. Consequently, the magnitudes of v'/U_J are comparable to those of u'/U_J in the lower jet in the recirculation region corresponding to $X/D \leqslant 7.76$. However, u'/U_J in the further downstream region is much stronger than v'/U_J because of the turbulent kinetic energy generated by the streamwise mean velocity as can be seen in the governing equation for the Reynolds normal stress for the two-dimensional shear flow.

Heat transfer characteristics

The local Nusselt number distributions along the plate are presented in the Fig. 7 for eight offset ratios and one Reynolds number of $Re = 39\,000$. In general,

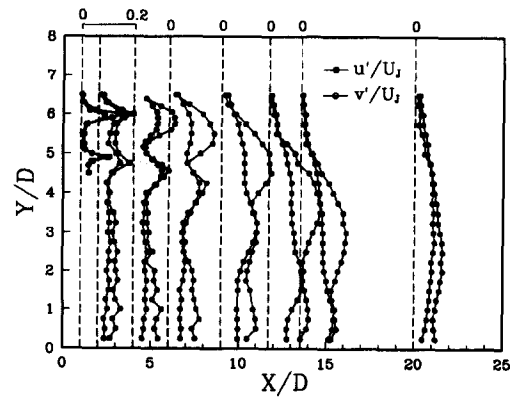

Fig. 6. Turbulent intensity profiles in the WAOJ for $H/D = 5.0$ and $Re = 39\,000$.

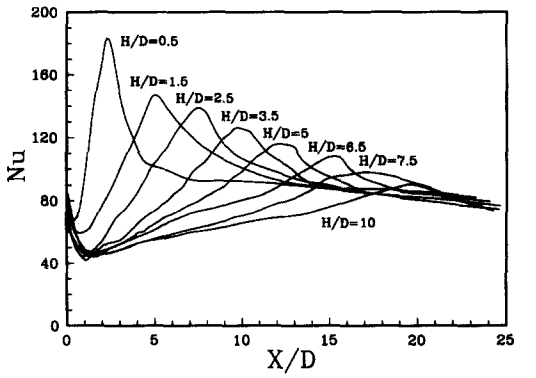

Fig. 7. Streamwise variations of the local Nusselt number with offset ratio for $Re = 39\,000$.

the local Nusselt number in the recirculation region increases due to turbulent mixing processes by the recirculation bubble and reaches a maximum value at the point where the jet flow reattaches. The Nusselt number in the wall jet region begins to decrease monotonically from the maximum value at the reattachment point and converges to nearly the same value at $X/D \approx 24$ as the flow redevelops far downstream. It should be noted that the minimum Nusselt number occurs between $X/D \approx 0.5$ and $X/D \approx 2.0$ for the offset ratios tested, with an increase of the Nusselt number as the upstream vertical wall is approached. This increase of the Nusselt number is attributed to an additional mixing of the flow caused by a secondary recirculation in the upstream corner near the step of the vertical wall. The existence of the secondary recirculation is also evidenced in Fig. 4 as well as observed by the color display of liquid crystal on the plate wall.

Figure 8 shows that for $Re = 39\,000$, both of the minimum and the maximum Nusselt number locations shift progressively downstream from $X/D \approx 0.5$–2.0 and from $X/D \approx 2.5$–20, respectively, as the offset ratio is raised from $H/D = 0.5$ to 12.5, and are well correlated by the following expressions:

$$X_{\min}/D = 0.63(H/D)^{0.45} \tag{3}$$

and

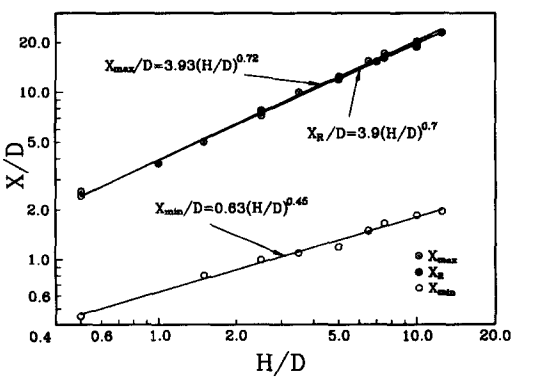

Fig. 8. Effect of the offset ratio on the maximum and minimum Nusselt number position, and reattachment length for $Re = 39\,000$.

$$X_{max}/D = 3.93(H/D)^{0.72}. \quad (4)$$

It should also be noted from Fig. 8 that the position of the time-averaged reattachment point coincides with the maximum Nusselt number position and has nearly the same dependency on the offset ratio as the maximum Nusselt number position (i.e. $X_R/D = 3.9(H/D)^{0.7}$). Vogel and Eaton [16], and Baughn *et al.* [17] have convincingly shown in the backward-facing step flow and in the round abrupt expansion flow, respectively, that the maximum Nusselt number position closely agrees with the reattachment point, and in the light of the close similarity of the flows, it can be assumed that the same is true for the WAOJ.

A variation of the maximum Nusselt number, Nu_{max}, with jet Reynolds number is shown in Fig. 9 for one offset ratio of $H/D = 5.0$ and the maximum Nusselt number varies according to $Nu_{max} \propto (Re)^{0.49}$. The reattachment point formed by the WAOJ can be considered to be the stagnation point in the impinging jet. Therefore, our result agrees closely with the laminar boundary layer result for the impinging jet flow which yields $Nu_{stag} \propto (Re)^{0.5}$. Kumada *et al.* [6] have reported in their mass transfer study with WAOJ that the maximum Sherwood number depends on $Re^{0.58}$ for the offset ratios ranging from 2.5 to 24.5.

The WAOJ flow is divided at the reattachment point, a part of the fluid flows reverse to the recirculation region and the rest of the fluid flows downstream in the wall jet region. Therefore, the flow and heat transfer characteristics in these two regions are different from each other. In order to investigate the heat transfer characteristics for these two different flow regimes, the following dimensionless length X^+ is defined.

$$X^+ = (X - X_{max})/X_{max}. \quad (5)$$

Figure 10 shows that for $H/D = 5.0$, the local Nusselt number distributions in the recirculation region corresponding to $X^+ \leqslant$ are correlated with Re and X^+ as

$$Nu = 0.691 Re^{0.49} \exp(1.114X^+). \quad (6)$$

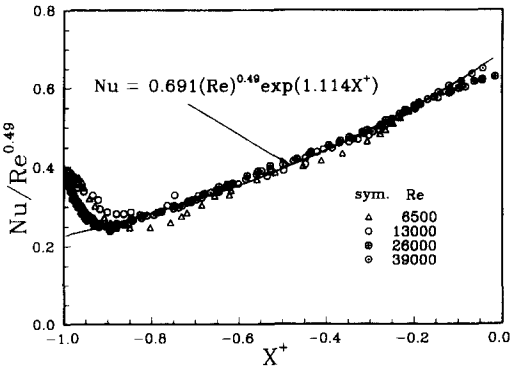

Fig. 10. Dependence of heat transfer parameter $Nu/Re^{0.49}$ on the dimensionless length X^+ in the recirculation region for $H/D = 5.0$.

On the other hand, the Nusselt number distributions in the redevelopment region corresponding to $X^+ > 0$ are shown in Fig. 11 and have the following correlation:

$$Nu = 0.201 Re^{0.56} X^{+(-0.135)}. \quad (7)$$

CONCLUSIONS

The flow characteristics such as reattachment phenomena, mean velocity and turbulence intensity profiles, and the effects of the Reynolds number and offset ratio on the heat transfer from a uniformly heated plate to the wall attaching offset jet (WAOJ) have been studied. It is observed that the WAOJ flow unstably reattaches in the impingement region and the reattachment region is rather wide and the minimum reattachment region occurs in the vicinity of $H/D = 7$ for $Re = 39\,000$. Although an initial development of the WAOJ is strongly affected by the suction pressure field in the recirculation region, the maximum velocity decay, the jet spread and the turbulence field in the wall jet region are similar to those of the plane wall jet. It is found that the maximum Nusselt number point coincides with the time-averaged reattachment point and the Nusselt number decreases mono-

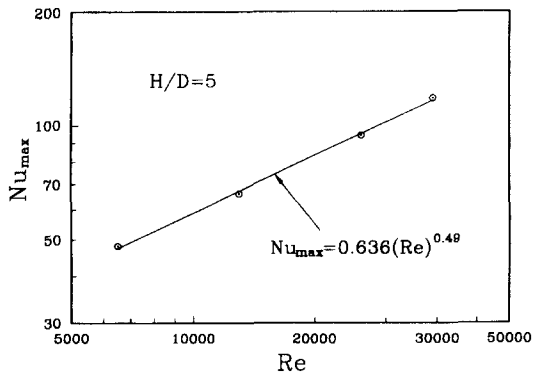

Fig. 9. Effect of Reynolds number on the maximum Nusselt number for $H/D = 5.0$.

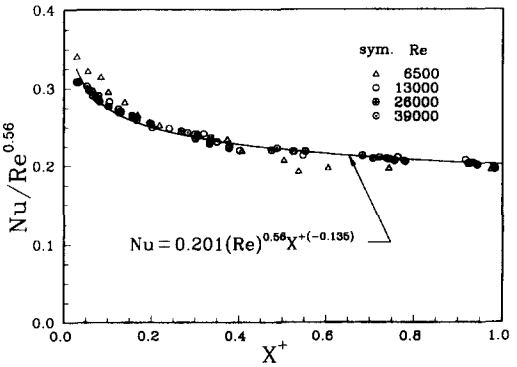

Fig. 11. Dependence of the heat transfer parameter $Nr/Re^{0.56}$ on the dimensionless length X^+ in the redevelopment region for $H/D = 5.0$.

tonically in the redevelopment region after the jet reattachment. The results also show an increase in the Nusselt number near the upstream corner region, suggesting the existence of a secondary vortex which causes an additional mixing of the flow. Both the minimum and maximum Nusselt number locations shift progressively downstream as the offset ratio is raised and are well correlated with the offset ratio. For $H/D = 5.0$, the maximum Nusselt number varies according to $Nu_{max} \propto Re^{0.49}$ which represents a weaker dependence on the Reynolds number than for the impinging jet flow. This may be attributed to a weaker momentum of the WAOJ flow compared to that of the impinging jet flow.

REFERENCES

1. C. Borque and G. Newmann, Reattachment of a two-dimensional incompressible jet to an adjacent flat plate, *Aerion Quat.* **11,** 201–232 (1960).
2. R. A. Sawyer, Two-dimensional reattachment jet flows inlcuding the effect of curvature on entrainment, *J. Fluid Mech.* **17,** 481–498 (1963).
3. J. Hoch and M. Jiji, Two-dimensional turbulent offset jet boundary interaction, *J. Fluids Engng* **103,** 154–161 (1981).
4. J. R. R. Pelfray and J. A. Liburdy, Mean flow characteristics of a turbulent offset jet, *J. Fluids Engng* **108,** 82–88 (1986).
5. S. H. Yoon, K. C. Kim, D. S. Kim and M. K. Chung, Comparative study of a turbulent wall-attaching offset jet and a plane wall jet, *Trans. KSME J.* **7,** 101–112 (1993).
6. M. Kumada, I. Mabuchi and K. Oyakawa, Studies in heat transfer to turbulent jets with adjacent boundaries (3rd report mass transfer to plane turbulent jet reattachment on an offset parallel plate), *Bull. JSME* **16,** 1712–1722 (1973).
7. J. Hoch and M. Jiji, Theoretical and experimental temperature distribution in two-dimensional turbulent jet-boundary interaction, *J. Heat Transfer* **103,** 331–336 (1981).
8. J. T. Holland and J. A. Liburdy, Measurements of the thermal characteristics of heated offset jet, *Int. J. Heat Mass Transfer* **33,** 69–78 (1990).
9. S. H. Yoon, Investigation on the turbulence structure of a wall-attaching offset jet, Ph.D. Thesis, Korea Advanced Institute of Science and Technology, Taejeon (1992).
10. S. J. Lee, J. H. Lee and D. H. Lee, Local heat transfer measurements from an elliptic jet impinging on a flat plate using liquid crystal, *Int. J. Heat Mass Transfer* **37,** 967–976 (1994).
11. K. Kim, A new hue-capturing technique for the quantitative interpretation of liquid crystal images used in convective heat transfer studies, Ph.D. Thesis, The Pennsylvania State University, PA (1991).
12. S. H. Ra, P. K. Chang and S. O. Park, A modified calibration technique for the split film sensor, *Meas. Sci. Technol.* **1,** 1156–1161 (1990).
13. S. J. Kline and F. A. McKlintock, Describing uncertainties in single sample experiments, *Mech. Engng* **5,** 3–8 (1953).
14. J. W. Baughn and S. Shimizu, Heat transfer measurements from a surface with uniform heat flux and an impinging jet, *J. Heat Transfer* **111,** 1096–1098 (1989).
15. N. Rajaratnam and N. Subramanya, Plane turbulent reattached wall jet, *J. Hydraulic Div.* **94,** 95–112 (1968).
16. J. C. Vogel and J. K. Eaton, Combined heat transfer and fluid dynamic measurements downstream of a backward-facing step, *J. Heat Transfer* **107,** 992–929 (1985).
17. J. W. Baughn, M. A. Hoffman, B. E. Launder, D. Lee and C. Yap, Heat transfer, temperature and velocity measurements downstream of an abrupt expansion in a circular tube at a uniform wall temperature. *J. Heat Transfer* **111,** 870–876 (1989).